

**Bradykinin restores left ventricular function, sarcomeric protein phosphorylation and e/nNOs levels in dogs with Duchenne muscular dystrophy cardiomyopathy**

**Running title: Cardiac effects of bradykinin in GRMD dogs**

Jin Bo Su<sup>1</sup>, Olivier Cazorla<sup>2</sup>, Stéphane Blot<sup>3</sup>, Nicolas Blanchard-Gutton<sup>3</sup>, Younss Ait Mou<sup>2</sup>, Inès Barthélémy<sup>3</sup>, Lucien Sambin<sup>1</sup>, Carolina Carlos Sampedrano<sup>1</sup>, Vassiliki Gouni<sup>1</sup>, Yves Unterfinger<sup>3</sup>, Pablo Aguilar<sup>3</sup>, Jean-Laurent Thibaud<sup>3</sup>, Alain Bizé<sup>1</sup>, Jean-Louis Pouchelon<sup>1</sup>, Hubert Dabiré<sup>1</sup>, Bijan Ghaleh<sup>1,4</sup>, Alain Berdeaux<sup>1,4</sup>, Valérie Chetboul<sup>1</sup>, Alain Lacampagne<sup>2</sup>, Luc Hittinger<sup>1,4</sup>

<sup>1</sup>Inserm, U955, Créteil, 94000, France;

<sup>2</sup>Inserm U1046, Université Montpellier1, Université Montpellier2, Montpellier, 34295, France;

<sup>3</sup>Université Paris-Est, Ecole Nationale Vétérinaire d'Alfort, UPR de Neurobiologie, Maisons-Alfort, 94700, France;

<sup>4</sup>Université Paris-Est, Faculté de Médecine, Créteil, 94000, France

Correspondence: Jin Bo Su, PhD  
INSERM U955, ENVA  
7 avenue du Général de Gaulle  
94700 Maisons-Alfort  
France  
Phone: 33-1-43967386  
Fax: 33-1-43967399  
Email: [jin-bo.su@inserm.fr](mailto:jin-bo.su@inserm.fr)

Total word count: 6488

**Bradykinin restores left ventricular function, sarcomeric protein phosphorylation and e/nNOs levels in dogs with Duchenne muscular dystrophy cardiomyopathy**

Jin Bo Su, Olivier Cazorla, Stéphane Blot, Younss Ait Mou, Nicolas Blanchard-Gutton, Inès Barthélémy, Lucien Sambin, Carolina Carlos Sampedrano, Vassiliki Gouni, Yves Unterfinger, Pablo Aguilar, Jean-Laurent Thibaud, Bijan Ghaleh, Alain Bizé, Jean-Louis Pouchelon, Hubert Dabiré, Alain Berdeaux, Valérie Chetboul, Alain Lacampagne, Luc Hittinger

**Abstract**

**Aims** Cardiomyopathy is a lethal result of Duchenne muscular dystrophy (DMD) but its characteristics remain elusive. The golden retriever muscular dystrophy (GRMD) dogs produce DMD pathology and mirror DMD patient's symptoms including cardiomyopathy. We previously showed that bradykinin slows the development of pacing-induced heart failure. Therefore, the goals of this research were to characterize dystrophin-deficiency cardiomyopathy and to examine cardiac effects of bradykinin in GRMD dogs

**Methods and results** At baseline, adult GRMD dogs had reduced fractional shortening ( $28\pm 2\%$  vs  $38\pm 2\%$  in control dogs,  $p<0.001$ ) and left ventricular (LV) subendocardial dysfunction leading to impaired endo-epicardial gradient of radial systolic velocity ( $1.3\pm 0.1$  cm/s vs  $3.8\pm 0.2$  cm/s in control dogs,  $p<0.001$ ) measured by echocardiography. These changes were normalized by bradykinin infusion ( $1 \mu\text{g}/\text{min}$ , 4 weeks). In isolated permeabilized LV subendocardial cells of GRMD dogs, tension-calcium relationships were shifted downward and force-generating capacity and transmural gradient of myofilament length-dependent activation were impaired compared with control dogs. Concomitantly, phosphorylation of sarcomeric regulatory proteins and levels of endothelial and neuronal nitric oxide synthase in LV myocardium were significantly altered in GRMD dogs. All these abnormalities were normalized in bradykinin-treated GRMD dogs.

**Conclusions** Cardiomyopathy in GRMD dogs is characterized by profound LV subendocardial dysfunction, abnormal sarcomeric protein phosphorylation and impaired endothelial and neuronal nitric oxide synthase, which can be normalized by bradykinin treatment. These data provide new insights into pathophysiological mechanisms accounting for DMD cardiomyopathy and open new therapeutic perspectives.

**Key words:** Duchenne muscular dystrophy cardiomyopathy; Myofilament Ca<sup>2+</sup> sensitivity; Protein phosphorylation; Nitric oxide synthase; Bradykinin

## Introduction

Duchenne muscular dystrophy (DMD) affects 1 in 3,500 male births and is the most prevalent X-linked genetic disorder. Cardiac involvement evolves towards cardiomyopathy with dilatation of the chambers and depression of left ventricular (LV) function. It is responsible for death in approximately 40% of patients aged between 10 and 30 years.<sup>1-3</sup> However, the characteristics of dystrophin-deficiency cardiomyopathy remain to be explored. Since the late 1980's, the golden retriever muscular dystrophy (GRMD) dogs have been used as the most relevant model of DMD<sup>4-6</sup> in preclinical investigations including drug treatment,<sup>6</sup> gene transfers<sup>7</sup> and cell therapy.<sup>5</sup> Similar to DMD patients, GRMD dogs also develop lethal cardiomyopathy.<sup>6,8</sup> The *mdx* mouse model is classically used for pathophysiological and therapeutic investigations. Nonetheless, compared to DMD patients and dogs, *mdx* mice present mild muscle pathology due to the upregulation of the dystrophin homolog utrophin<sup>9</sup> whereas this mechanism does not exist in GRMD dogs<sup>6</sup> and utrophin expression increases with the age and correlates with disease severity in DMD patients.<sup>10</sup> In addition, regional myocardial function is almost impossible to assess in *mdx* mice due to the small heart size and high heartbeat. Because GRMD dogs present severe skeletal muscle pathology and clinical symptoms similar to DMD,<sup>4-8</sup> this study was designed to characterize DMD cardiomyopathy in GRMD dogs with a special focus on regional contractile properties both *in vivo* and *in vitro*.

Previous studies showed that in dogs with pacing-induced cardiomyopathy, endogenous bradykinin exerted cardioprotective effects<sup>11</sup> and was involved in beneficial effects of angiotensin-converting enzyme inhibitors.<sup>12</sup> Moreover, in the same model, a bradykinin analogue improved LV endocardial flow reserve<sup>13</sup> and we showed that the progression of heart failure was prevented by early bradykinin administration.<sup>14</sup> However, the curative effect of bradykinin has never been evaluated in any model of established heart

failure. Thus, the present study attempted to address this question in GRMD dogs with apparent cardiomyopathy.

## Methods

### Animal model and experimental protocol

The animal care and the experimental protocol were in accordance with the Directive 2010/63/EU of the European Parliament and approved by the Animal Ethic Committee of Institut National de la Santé et de la Recherche Médicale.

In a preliminary echocardiographic study, fractional shortening in 3 normal golden retriever dogs (12 month-old), 4 GRMD dogs (9-12 month-old) and 4 younger GRMD dogs (<9 months) was 37.0-42.3%, 22.7-33.9% and 36.0-40.0%, respectively. Accordingly, criteria for the enrollment of GRMD dogs in the study were: age  $\geq 9$  months and fractional shortening  $\geq 25\%$  and  $\leq 35\%$ .

Fourteen GRMD dogs (CEDS, Mézilles, France) were instrumented with catheters in the left atrium and in the thoracic descending aorta during a left thoracotomy under general anesthesia induced with propofol (6.5 mg/kg, i.v.) and maintained with isoflurane (1-3% vol in 100% O<sub>2</sub>). The adequacy of anaesthesia was monitored by examination of animal reaction to pain stimulation. Preemptive and postoperative analgesia was ensured with morphine (0.1 mg/kg, i.v.) and fentanyl (50  $\mu$ g/h). After 2-3 weeks of recovery (Figure 1a), echocardiographic measurements were performed. Thereafter, pyrogen-free 0.9% saline (166  $\mu$ l/min) or bradykinin (NewMPS, France; dissolved in pyrogen-free 0.9% saline solution, 1  $\mu$ g/min, 166  $\mu$ l/min) was infused through the left atrial catheter for 4 weeks using a portable pump. The dose of bradykinin was chosen according to our previous studies showing that it slows the progression of heart failure without affecting arterial pressure.<sup>14,15</sup> Unchanged arterial pressure during bradykinin treatment was confirmed in the present study (Supplementary data). After sacrifice (pentobarbital, 100 mg/kg), cardiac tissues were collected for myocyte study and frozen with liquid nitrogen and stored at -80°C for protein analysis.

Among the 14 GRMD dogs, 3 died of acute respiratory failure following food inhalation, bronchopneumonia or gastric ulcers during postoperative recovery period, and 1 died of pulmonary hemorrhage during saline infusion. Finally, 10 GRMD and 8 age-matched normal golden retriever dogs of same genetic background were randomized.

Detailed echocardiography, myocyte experiments and Western blot analysis are described in supplementary data. Briefly, conventional echocardiography and 2D color tissue Doppler imaging were performed by the examiners blinded to the animals' group information. Myocytes were prepared from LV subendocardial and subepicardial strips and force-calcium relationships were examined in permeabilized myocytes.<sup>16,17</sup> Western blot analyses were performed to measure neuronal and endothelial nitric oxide synthase (nNOS and eNOS), cardiac myosin-binding protein C (cMyBP-C), phosphorylated cMyBP-C (p-MyBP-C), cardiac troponin I (TnI), phosphorylated TnI (p-TnI), ventricular myosin light chain 2 isoforms (VLC2, VLC2\*) and phosphorylated forms (p-VLC2 and p-VLC2\*) in LV tissues. The NOS activity was assessed by measuring the rate of L-arginine to nitrite/nitrate conversion in tissue lysates using a colorimetric NOS assay kit (NB78, Oxford Biomedical Research, Inc) following the manufacture's instructions.

### **Statistical analysis**

Results were expressed as mean $\pm$ SEM. One-way ANOVA for repeated measures was used for intra-group studies (StatView software, Abacus Concepts Inc). Two-way ANOVA was performed for comparisons between groups and if there was a significant difference, Student-Newman-Keuls test was used to identify differences between means. When only two means were compared, an appropriate Student's t-test was used. Linear least-squares regression was performed to evaluate cause-effect relationships between e/nNOS protein levels or sarcomeric protein phosphorylation and functional changes observed in intact animal

and isolated myocytes as well as between sarcomeric protein phosphorylation and e/nNOS protein levels. A  $p < 0.05$  was considered significant.

## Results

### LV dysfunction and its normalization by bradykinin infusion in GRMD dogs

GRMD dogs had lower body weight, higher heart rate, greater LV end-diastolic diameter/body weight ratio and thinner LV free wall and interventricular septum than control dogs (Table 1). GRMD dogs exhibited major LV contractile dysfunction as revealed by reduced fractional shortening, LV free wall and interventricular septal wall thickenings (Figure 1b, c and d). LV dysfunction occurred essentially in the subendocardium as indicated by decreased systolic velocity in the subendocardium and conserved systolic velocity in the subepicardium, which resulted in a reduced endo-epicardial gradient of radial systolic velocity (Figure 1e). GRMD dogs had also a reduced mitral E/A (Table 1).

Before placebo or bradykinin infusion, there was no difference between the two groups of control dogs or between the two groups of GRMD dogs (Supplementary data). Figure 2a illustrates LV myocardial velocities in one GRMD dog before and 4 weeks after bradykinin infusion. Bradykinin treatment did not modify LV end-diastolic diameter/body weight ratio in control and GRMD dogs (Figure 2b). LV contractile dysfunction persisted throughout the protocol in placebo-treated GRMD dogs (Figure 2c and d), while bradykinin-treated GRMD dogs exhibited normal LV systolic performance as indicated by normalized fractional shortening and LV free wall systolic thickening after 2 and 4 weeks of bradykinin infusion (Figure 2c and d). This may be due to the increase in subendocardial systolic velocity (Figure 2e). The radial epicardial systolic velocity was unchanged (Figure 2f), resulting in a normalized endo-epicardial gradient of radial systolic velocity in these dogs (Figure 2g).

**Impaired contractile properties of LV subendocardial myocytes in GRMD dogs were normalized by bradykinin treatment**

The regional properties of the contractile machinery were investigated in permeabilized cardiomyocytes by establishing force-calcium relationships. In subendocardial myocytes, the forces generated at sub-maximal and maximal calcium activation at 1.9  $\mu\text{m}$  and 2.3  $\mu\text{m}$  sarcomere lengths were reduced in GRMD dogs (Figure 3a). In subepicardial myocytes, tension-pCa relationships were superimposable at each sarcomere length in control and GRMD dogs (Figure 3b). Maximal tensions generated at the two sarcomere lengths in subendocardial cells were lower in GRMD dogs than in control dogs (Figure 3c) but no difference was observed in subepicardial cells between GRMD and control dogs (Figure 3d). In subendocardial and subepicardial cells, stretching myocyte from short to long sarcomere length induced a leftward shift of the tension-pCa relationship (Figure 3e) and an increase in  $\text{pCa}_{50}$  (the pCa for half maximum activation), both indicating an increased myofilament  $\text{Ca}^{2+}$  sensitivity, which is referred to as the length-dependent activation and reflects the Frank-Starling mechanism at the cellular level. The myofilament  $\text{Ca}^{2+}$  sensitivity was higher only at 1.9  $\mu\text{m}$  sarcomere length in subendocardial cells of GRMD dogs than in control dogs (Figure 3e). The myofilament  $\text{Ca}^{2+}$  sensitivity in subepicardial cells was not different between control and GRMD dogs (Figure 3f). In control dogs,  $\Delta\text{pCa}_{50}$  was higher in subendocardial myocytes than in subepicardial myocytes, resulting in a transmural gradient of length-dependent activation (Figure 3g), reflecting a higher endocardial reserve of  $\text{Ca}^{2+}$  sensitivity in response to increased sarcomere length. This gradient was lost in GRMD dogs due to a reduced length-dependent activation in subendocardial cells. Thus, the properties of the contractile machinery were altered in subendocardial myocytes of GRMD dogs.

Bradykinin treatment thoroughly improved the properties of the contractile machinery in subendocardial cells of GRMD dogs (Figure 4a) as indicated by restoration of maximal

active tensions to levels of control dogs (Figure 4b). Bradykinin did not modify myofilament  $\text{Ca}^{2+}$  sensitivity in control dogs but reduced  $\text{pCa}_{50}$  at 1.9  $\mu\text{m}$  in subendocardial cells of GRMD dogs compared with placebo-treated ones. The myofilament  $\text{Ca}^{2+}$  sensitivity of subendocardial cells at both 1.9 and 2.3  $\mu\text{m}$  sarcomere lengths was lower in bradykinin-treated GRMD dogs than in bradykinin-treated control dogs (Figure 4c). The endo-epicardial gradient of  $\Delta\text{pCa}_{50}$  in bradykinin-treated GRMD dogs was not different from that of control dogs (Figure 4d), indicating a restoration of endo-epicardial length-dependent activation gradient in GRMD dogs.

### **Phosphorylation of cMyBP-C, TnI and VLC2 isoforms in LV myocardium of GRMD dogs is normalized by bradykinin administration**

Since sarcomeric protein phosphorylation regulates the properties of the contractile machinery, we analyzed phosphorylation levels of Ser<sup>282</sup> cMyBP-C, Ser<sup>23/24</sup> TnI and two VLC2 isoforms in LV tissues. p-MyBP-C levels were similar in subepicardial and subendocardial regions in control dogs and were not modified by bradykinin treatment (Figure 5a and b). Compared with control dogs, p-MyBP-C levels were decreased in subepicardial and subendocardial regions in GRMD dogs. In contrast, p-MyBP-C levels in bradykinin-treated GRMD dogs were not statistically different from those of control dogs (Figure 5a and b). The amount of non-phosphorylated TnI was not different between groups. In control dogs, p-TnI levels were not different between the subepicardium and subendocardium and were not modified by bradykinin treatment (Figure 5a and c). The p-TnI level in the subendocardium was higher in GRMD dogs than in control dogs, which was normalized by bradykinin treatment (Figure 5a and c). There was an inverse linear relationship between p-TnI levels and  $T_{\text{max}}$  at 1.9  $\mu\text{m}$  sarcomere length in the subendocardial cells (Figure 5d). VLC2 isoform phosphorylation levels were similar in subepicardial and

subendocardial regions in placebo- and bradykinin-treated control and GRMD dogs (Figure 5e and 5f). VLC2 phosphorylation level decreased significantly only in the subepicardium of bradykinin-treated GRMD dogs (Figure 5e and 5f). The p-VLC2\*/VLC2\* level was significantly lower in the subendocardium than in the subepicardium in control dogs. This endo-epicardial difference was lost in bradykinin-treated control dogs and in placebo-treated GRMD dogs due to increased p-VLC2\*/VLC2\* level in the subendocardium (Figure 5g). Bradykinin treatment in GRMD dogs decreased p-VLC2\*/VLC2\* in subepicardial and subendocardial regions (Figure 5g). An inverse linear relationship between subendocardial p-VLC2\*/VLC2\* levels and fraction shortening was described (Figure 5h). Altogether, the phosphorylation of sarcomeric regulatory proteins was mainly altered in the subendocardium of GRMD dogs and was reversed by bradykinin treatment.

#### **Reduced nNOS and eNOS level and NOS activity in LV myocardium of GRMD dogs and restoration by bradykinin treatment**

Dystrophin deficiency in skeletal muscles leads to a selective loss and delocalization of nNOS. We therefore explore nNOS and eNOS content in GRMD hearts. Figure 6a shows representative Western blots of nNOS and eNOS. In control dogs, nNOS protein levels were similar in subendocardial and subepicardial regions of placebo- or bradykinin-treated dogs. nNOS protein levels were lower in LV subendocardium and subepicardium of placebo-treated GRMD dogs than in those of control dogs (Figure 6a and b). In contrast, in bradykinin-treated GRMD animals, nNOS levels increased by 156% ( $p < 0.02$ ) in the subepicardium and 70% ( $p < 0.05$ ) in the subendocardium compared with placebo-treated GRMD dogs and reached similar levels of placebo- or bradykinin-treated control dogs.

eNOS levels were similar in LV subendocardium and subepicardium in control dogs and were not modified by bradykinin treatment. Compared with control dogs, eNOS levels

were significantly decreased by 66% and 77% in LV subendocardium and subepicardium of placebo-treated GRMD dogs, but were similar in both regions of bradykinin-treated GRMD dogs (Figure 6a and c). These data indicate a down-regulation of nNOS and eNOS in the left ventricle of GRMD dogs, which can be restored by bradykinin treatment.

There was an inverse linear relationship between p-VLC\* and eNOS levels in the subendocardium ( $r=-0.54$ ,  $p<0.05$ ) but not in the subepicardium. A linear relationship between p-cMyBP-C and nNOS levels was described in the subepicardium and subendocardium ( $r=0.70$ ,  $p<0.01$  and  $r=0.50$ ,  $p<0.05$ , respectively), suggesting a substantial cause-effect relationship between nNOS and cMyBP-C phosphorylation. There was no linear relationship between p-TnI levels and eNOS or nNOS in LV myocardium. Fractional shortening was linearly related to nNOS levels in the subendocardium (Figure 6d) and in the subepicardium ( $r=0.65$ ,  $p<0.005$ ). Endo-epicardial systolic velocity gradient was linearly related to nNOS levels in the subepicardium ( $r=0.8$ ,  $p<0.01$ ) and subendocardium (Figure 6e). Similar relationships between fractional shortening or endo-epicardial systolic velocity gradient and eNOS were observed. Changes in  $pCa_{50}$  in subendocardial cells were inversely related to subendocardial eNOS levels ( $r=-0.53$ ,  $p<0.05$ ) but not related to subendocardial nNOS levels.

In control dogs, the NOS activity was lower in the subendocardium than in the subepicardium ( $p<0.05$ ). This difference disappeared in bradykinin-treated control dogs. The NOS activity in LV myocardium was lower in GRMD dogs than in control dogs (Figure 6f). In contrast, NOS activity in the subepicardium and subendocardium were similar between bradykinin-treated GRMD dogs and placebo- or bradykinin-treated control dogs, indicating a restoration of NOS activity by bradykinin treatment. More importantly, NOS activity increased significantly by 166% in the subendocardium of bradykinin-treated GRMD dogs as compared with placebo-treated GRMD dogs.

## Discussion

This study demonstrated that LV dysfunction of GRMD dogs was characterized by a reduced LV endo-epicardial gradient of radial systolic velocity due to a pronounced subendocardial dysfunction. This was related to altered myofibrillar properties in subendocardial cells and disappearance of transmural gradient of myofilament length-dependent activation. These changes were associated with altered cMyBP-C, TnI and VLC2\* phosphorylation as well as reduced nNOS and eNOS in LV myocardium. Moreover, our data showed that chronic bradykinin treatment normalized LV performance as indicated by normalized LV wall thickening and fractional shortening, and restored subendocardial function and endo-epicardial systolic velocity gradient. This *in vivo* effect of bradykinin was reflected at the cellular level by normalized myofibrillar properties of subendocardial cells.

In GRMD dogs, subendocardial dysfunction occurred even before LV global dysfunction,<sup>8</sup> leading to a loss of transmural contractile gradient. This loss is highlighted by the disappearance of endo-epicardial systolic velocity gradient, resulting in overall LV dysfunction. Concomitantly, subendocardial myocytes exhibited decreased capacity to generate force, increased  $Ca^{2+}$  sensitivity at short sarcomere length and abolished endo-epicardial length-dependent activation gradient that reduced the capacity of subendocardial cells to use the Frank-Starling mechanism when necessary<sup>18</sup> The preferential alteration of subendocardium compared with subepicardium has been described for various cardiac pathologies<sup>18</sup> This may relay on functional differences between subepicardial and subendocardial layers. A normal heart displays a LV transmural contractile gradient due to higher contractility in the subendocardium than in the subepicardium, resulting from the transmural excitation-contraction coupling heterogeneity<sup>19</sup> and higher sarcoplasmic reticulum  $Ca^{2+}$  release in the subendocardium than in the subepicardium.<sup>20</sup> The subendocardium has higher blood flow<sup>21</sup> and oxygen consumption<sup>22</sup> than the subepicardium. During systole and

diastole, vessel patency remains constant at the subepicardium, while during systole, subendocardial layers suffer transient ischemia due to low blood flow which requires compensatory replenishment from diastolic perfusion.<sup>23</sup> These features result in greater susceptibility of subendocardial layers than subepicardial layers to be dysfunctional in many circumstances. Additionally, the subepicardium can adapt to increased stress by lengthening the action potential to release more calcium. This adaptation is limited in subendocardial cells that have long action potential duration in basal conditions. In GRMD dogs, heart rate was accelerated. This shortened diastolic time and altered compensatory replenishment from diastolic perfusion needed for subendocardial cells. Moreover, changes in phosphorylation of sarcomeric regulatory proteins such as TnI and VLC2\* in the subendocardium of GRMD dogs indicate functional maladaptation.

cMyBP-C phosphorylation increases the force generation by accelerating the kinetics of force development through increasing the proximity of cross-bridges to actin<sup>24</sup> and cross-bridge kinetics.<sup>25</sup> When dephosphorylated, cMyBP-C interacts with myosin to prevent actin-myosin interaction, reducing  $Ca^{2+}$ -activated force generation.<sup>25,26</sup> A reduced cMyBP-C phosphorylation seems to be a common mechanism for human dilated and ischemic cardiomyopathy and canine pacing-induced cardiomyopathy.<sup>27</sup> Such mechanism also occurs in GRMD dogs and underlies reduced force-generating capacity in GRMD dogs. Accordingly, restoration of cMyBP-C phosphorylation following bradykinin treatment should participate in normalizing force-generating capacity of subendocardial cells in GRMD dogs.

TnI phosphorylation by protein kinase A reduces myofilament  $Ca^{2+}$  sensitivity and increases cross-bridge cycling rate. This accelerates relaxation and increases force generation but increases energy cost.<sup>28</sup> TnI phosphorylation was unchanged or increased in rat myocardial infarction model<sup>16,17</sup> but decreased in human hypertrophic or dilated failing hearts.<sup>29,30</sup> In GRMD dogs, TnI phosphorylation was increased in the subendocardium but not

in the subepicardium. This pattern of TnI phosphorylation seems to be unique for the failing heart of GRMD dogs and might compensate for LV subendocardial dysfunction in GRMD dogs. However, the energy-consuming feature of such compensation would increase the workload of subendocardial cells and played a deleterious role as suggested by an inverse relationship between T<sub>max</sub> and p-TnI. Bradykinin-induced normalization of TnI phosphorylation in GRMD dogs may correct this deleterious effect. The effect of bradykinin on TnI phosphorylation can be mediated through activation of p21-activated kinase I, which then dephosphorylates TnI in cardiomyocytes.<sup>31</sup>

Myosin light chain 2 regulates myocardial contraction. Unphosphorylated VLC2 slows the kinetic of actomyosin cross-bridge formation. VLC2 phosphorylation relieves this action, increases myofilament Ca<sup>2+</sup> sensitivity and is implied in the length-dependent activation mechanism.<sup>16,32,33</sup> We found that beside unchanged VLC2 phosphorylation, GRMD dogs lost the endo-epicardial gradient of VLC2\* phosphorylation due to increased VLC2\* phosphorylation in the subendocardium. However, the altered pattern of VLC and VLC2\* phosphorylation in GRMD dogs was different from that reported in rat myocardial infarction model where a decreased VLC2 but not VLC2\* phosphorylation was observed<sup>16,17</sup> and in infarcted porcine myocardium where neither VLC2 nor VLC2\* phosphorylation was changed.<sup>34</sup> The increased VLC2\* phosphorylation may be responsible for the increased Ca<sup>2+</sup> sensitivity at short sarcomere length in subendocardial cells leading to reduced transmural length-dependent activation in GRMD dogs. Consistently, normalized VLC2\* phosphorylation by bradykinin explains the decreased Ca<sup>2+</sup> sensitivity at short sarcomere length in subendocardial cells of bradykinin-treated GRMD dogs.

In DMD patients, dystrophin deficiency in skeletal muscles leads to selective loss and delocalization of nNOS and reduced blood flow in skeletal muscles, accounting for muscle lesions.<sup>35,36</sup> However, there is no information about nNOS in the DMD heart. We found a

marked reduction of myocardial nNOS levels in GRMD dogs. This is in line with a study in *mdx* mice showing a decreased cardiac nNOS activity<sup>37</sup> and contrast with another showing unchanged myocardial nNOS levels in *mdx* mice at different ages.<sup>38</sup> Interestingly, increased myocardial nNOS expression and activity were found in patients with dilated cardiomyopathy.<sup>39</sup> Thus, dystrophin-deficiency cardiomyopathy in this regard differs from dilated cardiomyopathies of other etiologies. nNOS participates in the regulation of coronary blood flow<sup>40</sup> and intracellular Ca<sup>2+</sup> homeostasis through its action on Ca<sup>2+</sup> release channel and Ca<sup>2+</sup> handling proteins,<sup>41,42</sup> a decreased nNOS level may contribute to LV contractile dysfunction. Our study is the first one to demonstrate an impaired eNOS level in dystrophin-deficiency cardiomyopathy. eNOS derived-NO regulates myocardial blood perfusion and LV endocardial reserve,<sup>43</sup> myocardial O<sub>2</sub> consumption<sup>44</sup> and Ca<sup>2+</sup> release from ryanodine-receptor channels.<sup>41,45</sup> eNOS-derived NO enhances the Frank-Starling mechanism in the isolated heart,<sup>46</sup> and eNOS gene expression is depressed in the subendocardium of patients with dilated cardiomyopathy and correlated with LV stroke work.<sup>47</sup> Decreased myocardial eNOS levels may also account for LV dysfunction in GRMD dogs.

In control heart, bradykinin treatment improves LV contractility without significant effects on protein phosphorylation and eNOS and nNOS protein levels. This can be explained by the fact that in the control heart, eNOS and nNOS expression and myofilament protein phosphorylation are normal, and bradykinin is a vasodilator that can increase myocardial coronary perfusion by liberating eNOS and nNOS derived-NO. It has been shown that myocardial systolic velocity measured by tissue Doppler imaging is closely correlated with myocardial blood flow measured by the microsphere technique.<sup>48</sup> Accordingly, our data showed an increased myocardial systolic velocity in the subendocardium but not in the subepicardium after bradykinin infusion in control dogs. This mechanism may also contribute to the improvement of subendocardial function in GRMD dogs. However, since eNOS and

nNOS system and myofilament protein phosphorylation are altered in GRMD hearts, this mechanism would be functional after restoration of eNOS and nNOS system as well as responsiveness of cardiomyocytes.

Bradykinin is a full B2 agonist and exerts its actions essentially through B2 receptors constitutively presented in various tissues.<sup>49</sup> In endothelial cells, B2 receptor activation increases intracellular  $Ca^{2+}$  that activate eNOS to release NO and phospholipase A2 to produce arachidonic acid that is metabolized into prostacyclin or endothelium-derived hyperpolarizing factor.<sup>50</sup> Bradykinin releases NO by modulating eNOS phosphorylation/dephosphorylation.<sup>51,52</sup> This should be impaired when the eNOS level is reduced in the heart. One of our new findings is that bradykinin upregulated both nNOS and eNOS levels in the left ventricle of GRMD dogs. This was in accordance with the upregulation of e/nNOS in arterial vessels of GRMD dog.<sup>53</sup> This allowed bradykinin to enhance NO production leading to improved myocardial function. The mechanism by which bradykinin regulates eNOS and nNOS levels needs further investigation. A limitation of the NOS activity assay used here was that the activity as measured was not verified to be blockable by a NOS inhibitor. Finally, linear relationships between e/nNOS and specific sarcomeric protein phosphorylation and between e/nNOS or specific sarcomeric protein phosphorylation and functional changes in intact animals or in isolated cardiomyocytes suggest substantial cause-effect between related parameters.

In conclusion, this study extended our knowledge about dystrophin-deficiency cardiomyopathy, showing marked subendocardial contractile impairment, loss of endo-epicardial length-dependent activation gradient, altered phosphorylation of sarcomeric regulatory proteins and reduced myocardial eNOS and nNOS levels. Bradykinin treatment normalized these abnormalities and LV contractile performance in GRMD dogs. Although little is known about these aspects in DMD patients with cardiomyopathy, because of

etiological similarity between GRMD and DMD, abnormalities observed in GRMD may occur in DMD patients and the effects of bradykinin may be expected in DMD patients. Finally, our data suggest that sarcomeric protein and e/nNOS are potential targets for fighting DMD cardiomyopathy.

## **Funding**

This study was supported by the AFM (JBS and LH N°13031, OC N°11590, SB N°13802, N°14389, N°15208 and AL N°15083), the Région Languedoc Roussillon (AL, “Chercheur d’Avenir”), a grant from the Région Ile de France (CODDIM) and by the Ministère de l’Agriculture (France).

## **Acknowledgments**

We thank the Centre d’Elevage du Domaine des Souches for breeding the French GRMD colony. We thank Olivier Borie, Aurore Brindejont, Xavier Cauchois, Dimitri Dagios, Angélique Gouffier, Ingrid Gruyer and Emilie Monnet for their excellent daily cares to our canine patients. We thank the Unité Fonctionnelle d’Imagerie and the CAAST of ENVA for their support to the clinical follow-up of dogs. We thank Dr. Frank Giton for his technical assistance in measuring NOS activity.

**Conflict of Interest:** none declared

## Reference

1. Nigro G, Comi LI, Politano L, Bain RJ. The incidence and evolution of cardiomyopathy in Duchenne muscular dystrophy. *Int J Cardiol* 1990;**26**:271-277.
2. de Kermadec JM, Bécane HM, Chénard A, Tertrain F, Weiss Y. Prevalence of left ventricular systolic dysfunction in Duchenne muscular dystrophy: an echocardiographic study. *Am Heart J* 1994;**127**:618-623.
3. Mukoyama M, Kondo K, Hizawa K, Nishitani H. Life spans of Duchenne muscular dystrophy patients in the hospital care program in Japan. *J Neurol Sci* 1987;**81**:155-158.
4. Cooper BJ, Winand NJ, Stedman H, Valentine BA, Hoffman EP, Kunkel LM *et al.* The homologue of the Duchenne locus is defective in X-linked muscular dystrophy of dogs. *Nature* 1988;**334**:154-156.
5. Sampaolesi M, Blot S, D'Antona G, Granger N, Tonlorenzi R, Innocenzi A *et al.* Mesoangioblast stem cells ameliorate muscle function in dystrophic dogs. *Nature* 2006;**444**:574-579.
6. Townsend D, Turner I, Yasuda S, Martindale J, Davis J, Shillingford M *et al.* Chronic administration of membrane sealant prevents severe cardiac injury and ventricular dilatation in dystrophic dogs. *J Clin Invest* 2010;**120**:1140–1150.
7. Bartlett RJ, Stockinger S, Denis MM, Bartlett WT, Inverardi L, Le TT *et al.* In vivo targeted repair of a point mutation in the canine dystrophin gene by a chimeric RNA/DNA oligonucleotide. *Nat Biotechnol* 2000;**18**:615-622.

8. Chetboul V, Escriou C, Tessier D, Richard V, Pouchelon JL, Thibault H *et al.* Tissue doppler imaging detects early asymptomatic myocardial abnormalities in a dog model of Duchenne's cardiomyopathy. *Eur Heart J* 2004;**25**:1934-1939.
9. Kleopa KA, Drousiotou A, Mavrikiou E, Ormiston A, Kyriakides T. Naturally occurring utrophin correlates with disease severity in Duchenne muscular dystrophy. *Hum Mol Genet* 2006;**15**:1623-1628.
10. Matsumura K, Ervasti JM, Ohlendieck K, Kahl SD, Campbell KP. Association of dystrophin-related protein with dystrophin-associated proteins in mdx mouse muscle. *Nature* 1992;**360**:588-591.
11. Cheng CP, Onishi K, Ohte N, Suzuki M, Little WC. Functional effects of endogenous bradykinin in congestive heart failure. *J Am Coll Cardiol* 1998;**31**:1679-1686.
12. Barbe F, Su JB, Guyene TT, Crozatier B, Ménard J, Hittinger L. Bradykinin pathway is involved in the acute hemodynamic effects of enalaprilat in dogs with heart failure. *Am J Physiol* 1996;**270**:H1985-H1992.
13. Nikolaidis LA, Doverspike A, Huerbin R, Hentosz T, Shannon RP. Angiotensin-converting enzyme inhibitors improve coronary flow reserve in dilated cardiomyopathy by a bradykinin-mediated, nitric oxide-dependent mechanism. *Circulation* 2002;**105**:2785-2790.
14. Tonduangu D, Hittinger L, Ghaleh B, Le Corvoisier P, Sambin L, Champagne S *et al.* Chronic infusion of bradykinin delays the progression of heart failure and preserves vascular endothelium-mediated vasodilation in conscious dogs. *Circulation* 2004;**109**:114-119.

15. Su JB, Barbe F, Houel R, Guyene TT, Crozatier B, Hittinger L. Preserved vasodilator effect of bradykinin in dogs with heart failure. *Circulation* 1998;**98**:2911-2918.
16. Cazorla O, Szilagyi S, Le Guennec JY, Vassort G, Lacampagne A. Transmural stretch-dependent regulation of contractile properties in rat heart and its alteration after myocardial infarction. *FASEB J* 2005;**19**:88-90.
17. Ait Mou Y, Toth A, Cassan C, Czuriga D, de Tombe PP, Papp Z *et al.* Beneficial effects of SR33805 in failing myocardium. *Cardiovasc Res* 2011;**91**:412-419.
18. Cazorla O, Lacampagne A. Regional variation in myofilament length-dependent activation. *Pflugers Arch* 2011;**462**:15-28.
19. Furukawa T, Myerburg RJ, Furukawa N, Bassett AL, Kimura S. Differences in transient outward currents of feline endocardial and epicardial myocytes. *Circ Res* 1990;**67**:1287-1291.
20. Ait Mou Y, Reboul C, Andre L, Lacampagne A, Cazorla O. Late exercise training improves non-uniformity of transmural myocardial function in rats with ischaemic heart failure. *Cardiovasc Res* 2009;**81**:555–64.
21. Feigl EO. Coronary physiology. *Physiol Rev* 1983;**63**:1-205.
22. Weiss HR, Neubauer JA, Lipp JA, Sinha AK. Quantitative determination of regional oxygen consumption in the dog heart. *Circ Res* 1978;**42**:394–401.
23. Jan KM. Distribution of myocardial stress and its influence on coronary blood flow. *J Biomech* 1985;**18**:815-820.

24. Colson BA, Locher MR, Bekyarova T, Patel JR, Fitzsimons DP, Irving TC *et al.* Differential roles of regulatory light chain and myosin binding protein-C phosphorylations in the modulation of cardiac force development. *J Physiol* 2010;**588**:981-993.
25. Tong CW, Stelzer JE, Greaser ML, Powers PA, Moss RL. Acceleration of crossbridge kinetics by protein kinase A phosphorylation of cardiac myosin binding protein C modulates cardiac function. *Circ Res* 2008;**103**:974-982.
26. Kunst G, Kress KR, Gruen M, Uttenweiler D, Gautel M, Fink RH. Myosin binding protein C, a phosphorylation-dependent force regulator in muscle that controls the attachment of myosin heads by its interaction with myosin S2. *Circ Res* 2000;**86**:51-58.
27. El-Armouche A, Pohlmann L, Schlossarek S, Starbatty J, Yeh Y-H, Nattel S *et al.* Decreased phosphorylation levels of cardiac myosin-binding protein-C in human and experimental heart failure. *J Mol Cell Cardiol* 2007;**43**:223-229.
28. Layland J, Solaro RJ, Shah AM. Regulation of cardiac contractile function by troponin I phosphorylation. *Cardiovasc Res* 2005;**66**:12-21.
29. van der Velden J, Narolska NA, Lamberts RR, Boontje NM, Borbély A, Zaremba R *et al.* Functional effects of protein kinase C-mediated myofilament phosphorylation in human myocardium. *Cardiovasc Res* 2006;**69**:876-887.
30. Zhang J, Guy MJ, Norman HS, Chen Y-C, Xu Q, Dong X *et al.* Top-down quantitative proteomics identified phosphorylation of cardiac troponin I as a candidate biomarker for chronic heart failure. *J Proteome Res* 2011;**10**:4054-4065.

31. Ke Y, Sheehan KA, Egom EE, Lei M, Solaro RJ. Novel bradykinin signaling in adult rat cardiac myocytes through activation of p21-activated kinase. *Am J Physiol Heart Circ Physiol* 2010;**298**:H1283-H1289.
32. Venema RC, Raynor RL, Noland TA Jr, Kuo JF. Role of protein kinase C in the phosphorylation of cardiac myosin light chain 2. *Biochem J* 1993;**294**:401-406.
33. Pawloski-Dahm CM, Song G, Kirkpatrick DL, Palermo J, Gulick J, Dorn GW 2nd *et al.* Effects of total replacement of atrial myosin light chain-2 with the ventricular isoform in atrial myocytes of transgenic mice. *Circulation* 1998;**97**:1508-1513.
34. van der Velden J, Merkus D, Klarenbeek BR, James AT, Boontje NM, Dekkers DH *et al.* Alterations in myofilament function contribute to left ventricular dysfunction in pigs early after myocardial infarction. *Circ Res* 2004;**95**:e85-e95.
35. Thomas GD, Sander M, Lau KS, Huang PL, Stull JT, Victor RG. Impaired metabolic modulation of  $\alpha$ -adrenergic vasoconstriction in dystrophin-deficient skeletal muscle. *Proc Natl Acad Sci USA* 1998;**95**:15090-15095.
36. Sander M, Chavoshan B, Harris SA, Iannaccone ST, Stull JT, Thomas GD *et al.* Functional muscle ischemia in neuronal nitric oxide synthase-deficient skeletal muscle of children with Duchenne muscular dystrophy. *Proc Natl Acad Sci USA* 2000;**97**:13818-13823.
37. Bia BL, Cassidy PJ, Young ME, Rafael JA, Leighton B, Davies KE *et al.* Decreased myocardial nNOS, increased iNOS and abnormal ECGs in mouse models of Duchenne muscular dystrophy. *J Mol Cell Cardiol* 1999;**31**:1857-1862.

38. Wehling-Henricks M, Jordan MC, Roos KP, Deng B, Tidball JG. Cardiomyopathy in dystrophin-deficient hearts is prevented by expression of a neuronal nitric oxide synthase transgene in the myocardium. *Hum Mol Genet* 2005;**14**:1921-1933.
39. Damy T, Ratajczak P, Shah AM, Camors E, Marty I, Hasenfuss G *et al.* Increased neuronal nitric oxide synthase-derived NO production in the failing human heart. *Lancet* 2004;**363**:1365-1367.
40. Seddon M, Melikian N, Dworakowski R, Shabeeh H, Jiang B, Byrne J *et al.* Effects of neuronal nitric oxide synthase (nNOS) on human coronary diameter and blood flow in vivo. *Circulation* 2009;**119**:2656-2662.
41. Barouch LA, Harrison RW, Skaf MW, Rosas GO, Cappola TP, Kobeissi ZA *et al.* Nitric oxide regulates the heart by spatial confinement of nitric oxide synthase isoforms. *Nature* 2002;**416**:337-339.
42. Burger DE, Lu X, Lei M, Xiang FL, Hammoud L, Jiang M *et al.* Neuronal nitric oxide synthase protects against myocardial infarction-induced ventricular arrhythmia and mortality in mice. *Circulation* 2009;**120**:1345-1354
43. Jones CJ, Kuo L, Davis MJ, DeFily DV, Chilian WM. Role of nitric oxide in the coronary microvascular responses to adenosine and increased metabolic demand. *Circulation* 1995;**91**:1807-1813
44. Trochu JN, Bouhour JB, Kaley G, Hintze TH. Role of endothelium-derived nitric oxide in the regulation of cardiac oxygen metabolism: implications in health and disease. *Circ Res* 2000;**87**:1108-1117.

45. Petroff MG, Kim SH, Pepe S, Dessy C, Marbán E, Balligand JL *et al.* Endogenous nitric oxide mechanisms mediate the stretch dependence of Ca<sup>2+</sup> release in cardiomyocytes. *Nat Cell Biol* 2001;**3**:867-873.
46. Prendergast B, Sagach V, Shah A. Basal release of nitric oxide augments the Frank-Starling response in the isolated heart. *Circulation* 1997;**96**:1320-1329.
47. Heymes C, Vanderheyden M, Bronzwaer JG, Shah AM, Paulus WJ. Endomyocardial nitric oxide synthase and left ventricular preload reserve in dilated cardiomyopathy. *Circulation* 1999;**99**:3009-3016.
48. Derumeaux G, Ovize M, Loufoua J, Pontier G, André-Fouet X, Cribier A. Assessment of nonuniformity of transmural myocardial velocities by color-coded tissue doppler imaging: characterization of normal, ischemic, and stunned myocardium. *Circulation* 2000;**101**:1390-1395.
49. Su JB, Hoüel R, Héloire F, Barbe F, Beverelli F, Sambin L *et al.* Stimulation of bradykinin B1 receptors induces vasodilation in conductance and resistance coronary vessels in conscious dogs: comparison with B2 receptor stimulation. *Circulation* 2000;**101**:1848-1853.
50. Su JB. Kinins and cardiovascular diseases. *Curr Pharm Des* 2006;**12**:3423-3435.
51. Fleming I, Fisslthaler B, Dimmeler S, Kemp BE, Busse R. Phosphorylation of Thr495 regulates Ca(2+)/calmodulin-dependent endothelial nitric oxide synthase activity. *Circ Res* 2001;**88**:e68-e75.
52. Harris MB, Ju H, Venema VJ, Liang H, Zou R, Mitchell BJ *et al.* Reciprocal phosphorylation and regulation of endothelial nitric-oxide synthase in response to bradykinin stimulation. *J Biol Chem* 2001;**276**:16587-16591.

53. Dabiré H, Barthélémy I, Blanchard-Gutton N, Sambin L, Sampedrano CC, Gouni V *et al.* Vascular endothelial dysfunction in Duchenne muscular dystrophy is restored by bradykinin through upregulation of eNOS and nNOS. *Basic Res Cardiol* 2012;**107**:1-9.

## Figure Legends

Figure 1. Experimental protocol (a) and transventricular M-mode echocardiography at baseline showing decreased fractional shortening (FS), thinner LV wall thicknesses and hyperechoic lesions (arrows) within the LV free wall (LVFW) and interventricular septum (IVS) in GRMD dogs (b). (c), (d) and (e) Mean values of fractional shortening, LVFW and IVS wall systolic thickening and radial systolic velocities simultaneously recorded in subendocardial and subepicardial regions of LVFW and their difference (Endo-Epi gradient) in control and GRMD dogs. N= 8 and 14 for control and GRMD dogs. \* $p < 0.005$  vs control dogs.

Figure 2. Effects of bradykinin (BK) on LV contractile function in control and GRMD dogs. (a) Radial myocardial velocity profiles in a GRMD dog at day0 and 4 weeks after bradykinin infusion using 2D color tissue Doppler imaging. Myocardial velocities in subendocardial and subepicardial segments (yellow and green curves respectively) were recorded within the LVFW. Note increased systolic endo-epicardial gradient (red arrow) after bradykinin treatment owing to higher systolic subendocardial velocities. S, E, and A are the peak mean velocity of the LVFW during systole, early diastole, and late diastole, respectively. (b) No change in LV end-diastolic diameter normalized by body weight. (c), (d) and (e) Normalization of fractional shortening, LVFW thickening and radial systolic velocity in LV subendocardial regions of GRMD dogs after 2 and 4 weeks of bradykinin infusion. (f) No change in radial systolic velocity in LV subepicardial regions among groups. (g) Restoration of the endo-epicardial gradient of radial systolic velocity in bradykinin-treated GRMD dogs. N= 4, 4, 5 and 5 for control-placebo, control-bradykinin, GRMD-placebo and GRMD-bradykinin groups, respectively. \* $p < 0.05$  vs control-placebo and † $p < 0.05$  vs GRMD-placebo by ANOVA.

Figure 3. Mechanical properties of cardiomyocytes isolated from control and GRMD dogs. Tension-pCa curves were established at two sarcomere lengths (SL) in isolated permeabilized subendocardial (a) and subepicardial (b) myocytes of control and GRMD dogs. (c) Maximal active tension generated in subendocardial cells and (d) in subepicardial cells. (e) Myofilament  $\text{Ca}^{2+}$  sensitivity ( $\text{pCa}_{50}$ ) at two SL in subendocardial cells and (f) in subepicardial cells. (g) Transmural length-dependent activation measured by the difference of  $\text{pCa}_{50}$  between 2.3 and 1.9  $\mu\text{m}$  ( $\Delta\text{pCa}_{50}$ ) in subendocardial cells and subepicardial cells of control and GRMD dogs. Averaged data from 4 control and 5 GRMD dogs, and 3-4 cells per animal and region. \* $p < 0.05$ .

Figure 4. Effects of bradykinin on the contractile machinery properties in control and GRMD subendocardial myocytes. (a) Tension-pCa curves at two sarcomere lengths (SL) in subendocardial cells of bradykinin-treated control and GRMD dogs. (b) Normalized maximal tension in response to  $\text{Ca}^{2+}$  in subendocardial cells of bradykinin-treated control and GRMD dogs. (c)  $\text{pCa}_{50}$  at 1.9 or 2.3  $\mu\text{m}$  SL in subendocardial cells of placebo- or bradykinin-treated control and GRMD dogs. (d) The endo-epicardial gradient of  $\text{pCa}_{50}$  changes ( $\Delta\text{pCa}_{50}$ ) relative to SL change from 1.9  $\mu\text{m}$  to 2.3  $\mu\text{m}$  in response to  $\text{Ca}^{2+}$  in bradykinin-treated control and GRMD dogs. Endo: endocardial; Epi: epicardial. Averaged data from 4 control and 5 GRMD dogs in each condition, and 3-4 cells per animal and region. \* $p < 0.05$ .

Figure 5. Phosphorylation levels of sarcomeric regulatory proteins in subepicardial (Epi) and subendocardial (Endo) tissues. (a) Western blots of cMyBP-C, p-MyBP-C, troponin-I (TnI), p-troponin-I (p-TnI) and calsequestrin (Calsq) in placebo- or bradykinin (BK)-treated control and GRMD dogs. (b) Reduced p-MyBP-C/cMyBP-C in GRMD dogs and its normalization in

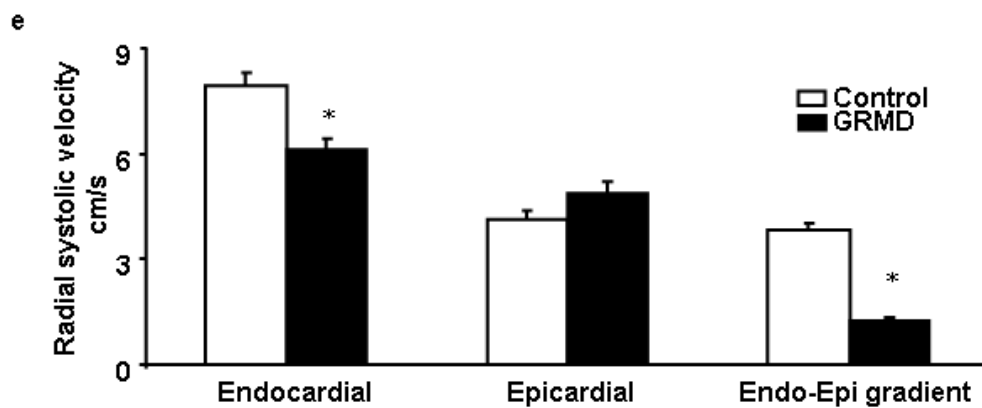
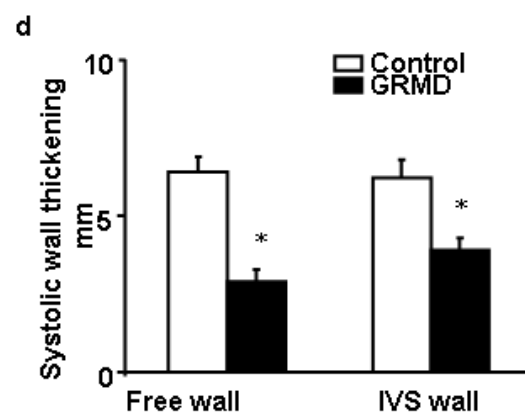
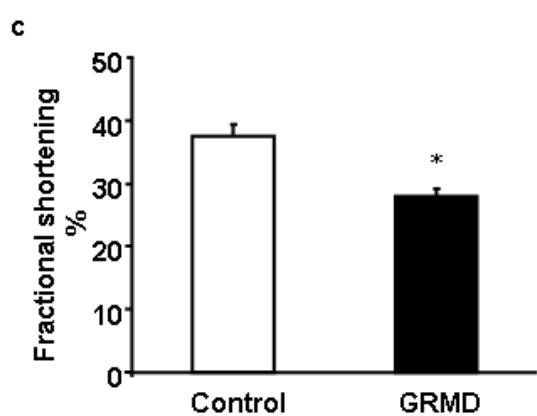
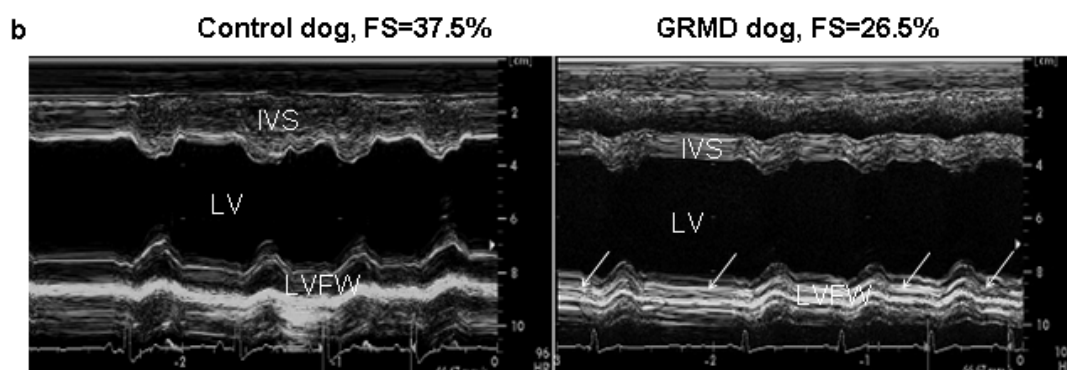
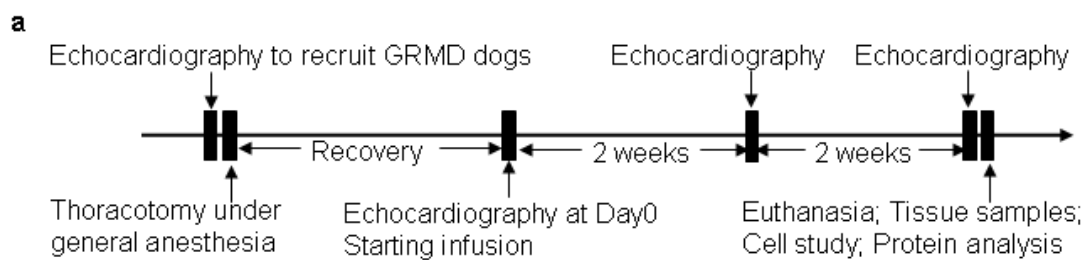
bradykinin-treated GRMD dogs. (c) Increased p-TnI/TnI in the subendocardium of GRMD but normalized p-TnI/TnI in bradykinin-treated GRMD dogs. (d) Linear relationship between T<sub>max</sub> obtained at 1.9 μm sarcomere length and p-TnI/TnI levels in subendocardial cells of placebo- and bradykinin-treated control and GRMD dogs. (e) Example of Western blot of VLC2, VLC2\* and their phosphorylated forms, p-VLC2 and p-VLC2\*. (f) No difference in p-VLC2 between control and GRMD dogs. (g) Increased p-VLC2\* level in the subendocardium of GRMD and bradykinin-treated control dogs but reduced in bradykinin-treated GRMD dogs. (h) Linear relationship between fractional shortening (FS) and subendocardial p-VLC2\*/VLC2\* levels in placebo- and bradykinin-treated control and GRMD dogs. Averaged data from 4 control and 5 GRMD dogs in each condition in duplicate. \*p<0.05 vs control dogs, † p<0.05 vs corresponding placebo-treated dogs, and ‡ p<0.05 vs the subepicardium.

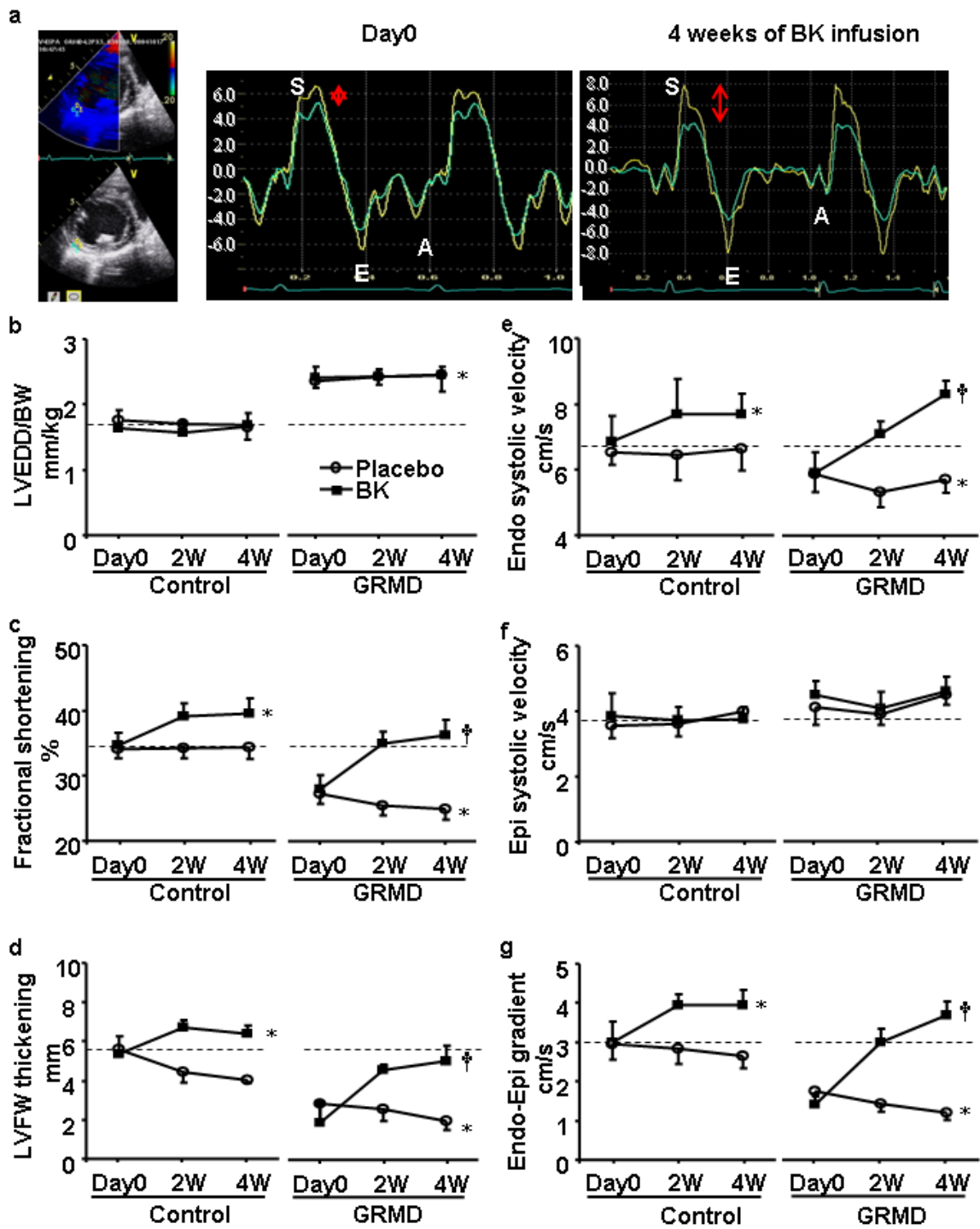
Figure 6. e/nNOS expression and NOS activity in control and GRMD dogs. (a) Example of Western blot of nNOS, eNOS and calnexin in LV subepicardium (Epi) and subendocardium (Endo) of placebo- or bradykinin-treated control and GRMD dogs. (b) and (c) Average values of nNOS and eNOS normalized by calnexin in the subendocardium and subepicardium. (d) Linear relationship between fractional shortening (FS) and subendocardial nNOS protein levels. (e) Linear relationship between endo-epicardial gradient of radial systolic velocity and subendocardial nNOS protein levels. (f) NOS activity measured by the rate of L-arginine to nitrite/nitrate conversion. Averaged data from 4 control and 5 GRMD dogs in each condition in duplicate. \*p<0.05 vs placebo-treated control dogs, †p<0.05 vs placebo-treated GRMD dogs.

Table 1. Echocardiographic data before surgical intervention in conscious control and GRMD dogs

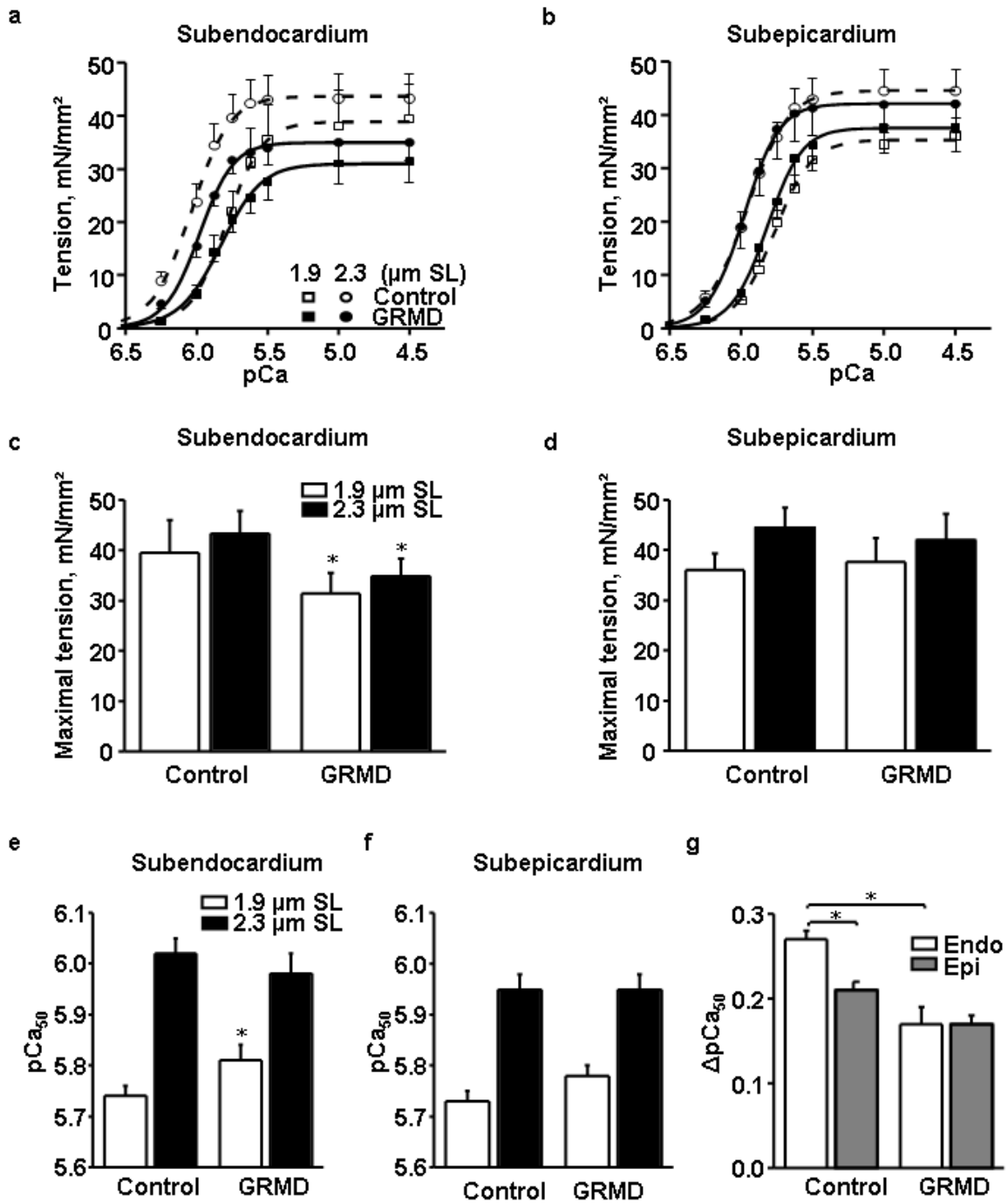
	Control dogs	GRMD dogs	p value of unpaired Student's t-test
N	8	14	
Age, months	12.2±0.4	10.8±1.1	ns
Body weight, kg	28.1±2.3	18.9±1.1	<0.0005
Heart rate, beats/min	101±11	127±5	<0.02
LVEDD, mm	46.7±2.0	41.2±1.6	<0.05
LVEDD/body weight, mm/kg	1.7±0.1	2.2±0.1	<0.005
LVESD, mm	29.1±1.2	29.6±1.0	ns
LV EDFWTh, mm	9.9±0.6	7.2±0.3	<0.0003
LV ESFWTh, mm	16.3±0.9	10.1±0.4	<0.0001
LV EDIVSWTh, mm	10.5±0.3	7.5±0.4	<0.00005
LV ESSWTh, mm	16.7±0.8	11.4±0.5	<0.00001
E/A mitral	1.9±0.2	1.5±0.1	<0.05

Data are presented as mean±SEM. LV, left ventricular; EDD, end-diastolic diameter; ESD, end-systolic diameter; EDFWTh, end-diastolic free wall thickness; ESFWTh, end-systolic free wall thickness; EDIVSWTh, end-diastolic interventricular septal wall thickness; ESIVSWTh, end-systolic interventricular septal wall thickness; E/A mitral, ratio of early to late diastolic mitral flow velocity.

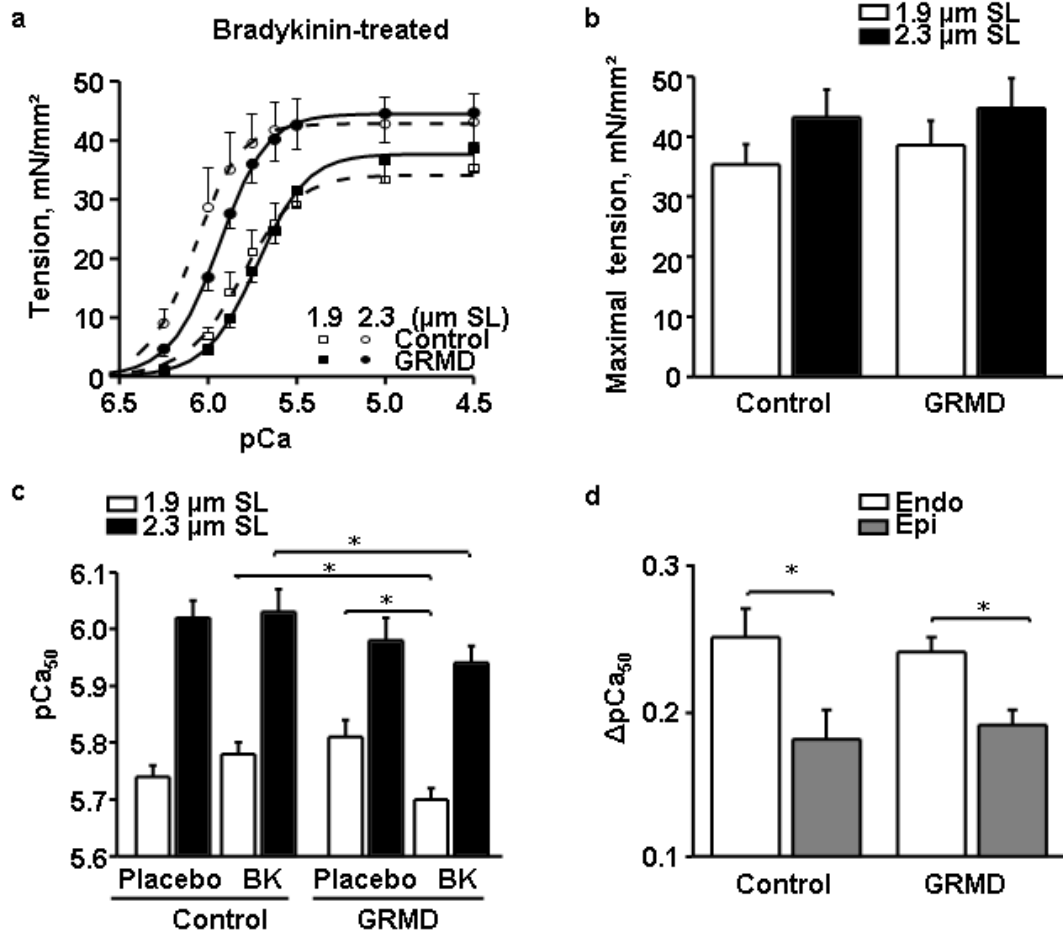




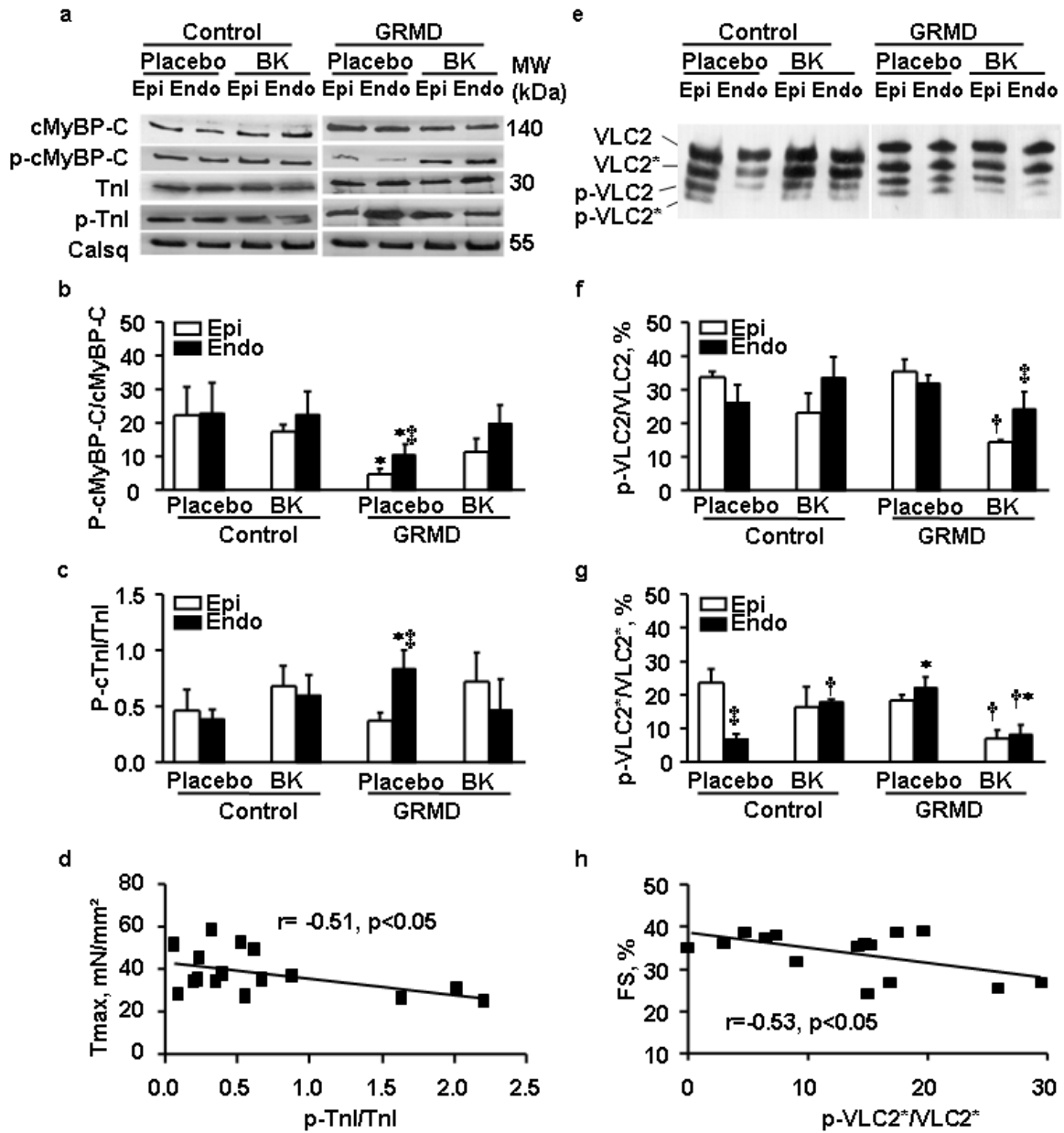
Su- Fig.2.



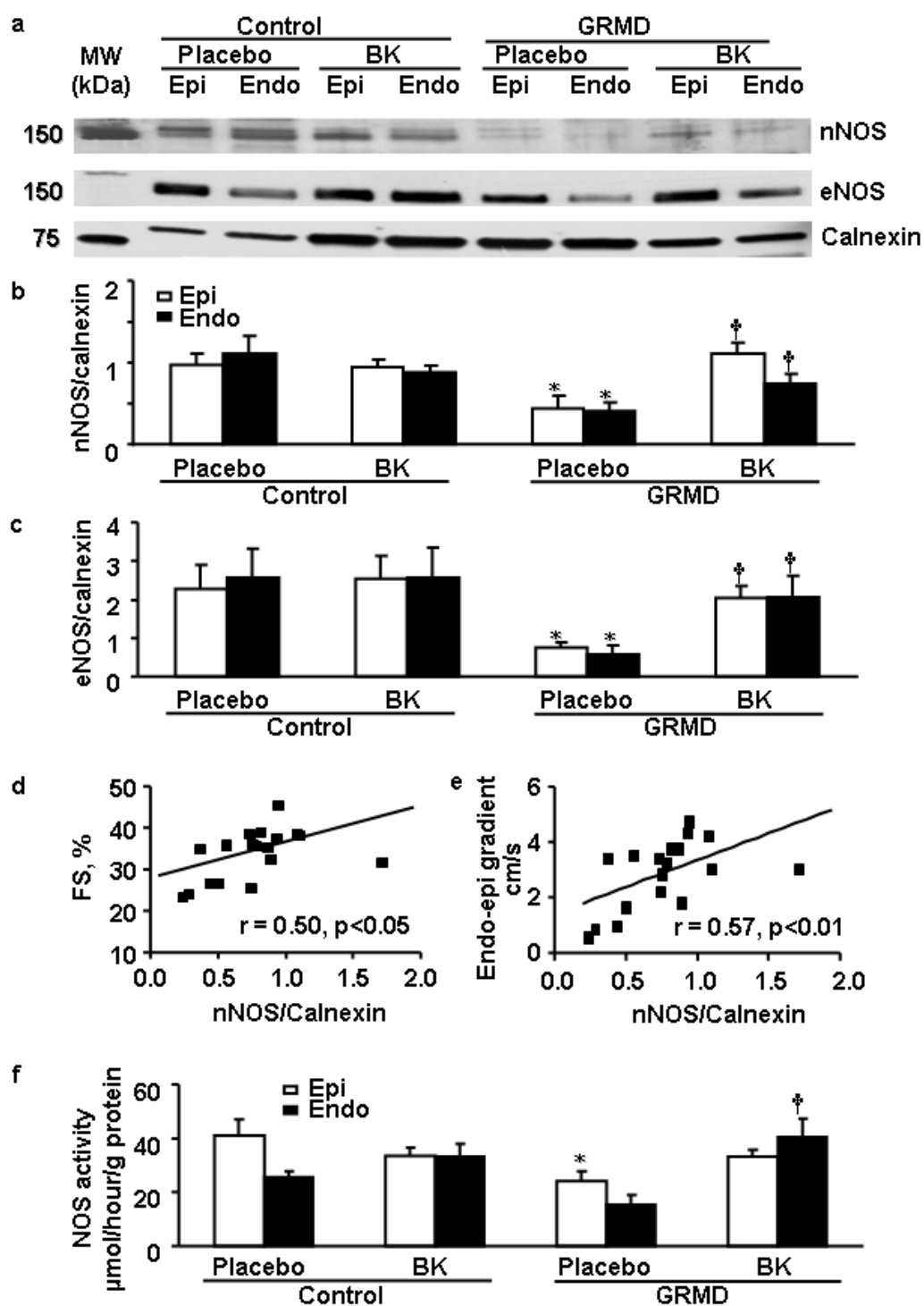
Su- Fig.3.



Su- Fig.4.



Su-Fig.5.



Su- Fig.6.